The Block Propagation in Blockchain-based Vehicular Networks

Xuefei Zhang, *Member, IEEE,* Wenbo Xia, Xiaochen Wang, *Member, IEEE,* Junjie Liu, Qimei Cui, *Senior Member, IEEE,* Xiaofeng Tao, *Senior Member, IEEE,* and Ren Ping Liu, *Senior Member, IEEE*

***Abstract*—Consensus is one of the most important issues of a blockchain system because it is a necessary process to reach an agreement between a group of separated nodes that do not trust each other in a decentralized framework. Most existing blockchain consensus works assume that the time of block propagation among separated nodes during the consensus process is ignorable, i.e., a block always successfully reaches every participating node during a period of time that is far shorter than the mining time. However, when blockchain is used in vehicular ad-hoc networks (VANET), the block propagation time is no longer negligible since the dynamic connectivity of the moving nodes in a wireless environment brings opportunistic communication to blockchain consensus. In this paper, we study the impact of mobility on block propagation under the single-chain structure in VANET. Specifically, we investigate the dynamics of block propagation from the macroscopic view and derive the closed-form expression of the single-block propagation time. Then, we characterize the blockchain forking as the multi-block competitive propagation. In this way, an approximate result on multi-block propagation time is discussed. An interesting finding is that higher mobility and more moving vehicles can speed up the block propagation. In addition, we also discover that distinct propagation capabilities of moving nodes contribute to the forking reduction in the blockchain consensus.**

***Index Terms*—Blockchain, block propagation, consensus, mobility, VANET.**

I. Introduction

THE goal of vehicular network is to improve traffic safety and efficiency by information exchanging between vehicles or with surrounding entities. Commonly, it operates in a centralized way which guarantees the credibility of information by an authoritative third party. In this way, the network breaks down once the single point of failure on centralized node happens [1]. In addition, network scalability is also a thorny issue in the centralized framework.

The blockchain technology seems the draw of the above problem in centralized framework. Blockchain is a promising and revolutionary technology for the decentralized framework. The whole point of using a blockchain is to let nodes, in particular nodes who do not trust one another, share valuable data in a secure way [2]. Considering the decentralized nature of blockchain, the networks in an ad-hoc way, such as Vehicular Ad-hoc Network (VANET), are potential scenarios for deploying blockchain. In addition, with the rapid development of vehicle intelligence and Internet of Vehicles (IoV) technology, a large number of vehicles have formed a huge distributed resource pool [3], which provides an environment support to employ blockchain system in vehicles. Moreover, vehicles as the members of IoV have the incentives to mutual supervision for improving the network performance. Noticeably, incentives to mutual supervision is the unique requirement of applying blockchain.

When blockchain is employed in the vehicles, i.e., vehicular blockchain in this paper, the dynamic topology incurred by vehicle moving results in the information exchange behaviors changing from the deterministic communications (in a fixed-wired network) to the opportunistic communications (in a wireless and dynamic network) [4]. In this condition, the block propagation time is no longer negligible, and even leading to the longer consensus time and forking, which has been a bottleneck for the vehicular blockchain.

Currently, one common idea to reduce the consensus time in blockchain is to replace the time-consuming proof of work (PoW) mechanism with the credit-based mechanism [5], such as proof of stake (PoS), delegated proof of stake (DPoS), proof of utility (PoU), and etc. In addition, directed acyclic graph (DAG) is utilized to reach a consensus in a parallel way to further reduce the consensus time [6]. Hence, the preliminary solutions to reduce consensus time mainly focus on the mechanism design itself.

Several studies analyze the consensus process concerning the impact of communication, including the investigations in [7] that prove the impact of network latency on blockchain consensus failure/forking. It also finds that the nodes with strong connectivity (communication) capability can gain an unfair advantage in terms of mining rewards. Moreover, the imperfect communication links in wireless blockchain system are discussed in [8,9,10]. Then, the failure of communication during consensus is proved an inducement to longer consensus time [11]. Hence, the time of the imperfect communication during the consensus is nonnegligible, especially for the mobile scenario where the information exchange between the nodes may fail due to the limited communication range over the wireless links and the highly dynamic communication topologies.

Motivated by the above observations, this paper aims to fill in the gap left by the previous work on vehicular blockchain consensus from the communication perspective,

X. Zhang, W. Xia, J. Liu, Q. Cui, and X. Tao are with the National Engineering Laboratory for Mobile Network Technologies, Beijing University of Posts and Telecommunications, Beijing 100876, China (e-mail: zhangxuefei@bupt.edu.cn; sarachocolate@bupt.edu.cn; junjieliu@bupt.edu.cn; cuiqimei@bupt.edu.cn; taoxf@bupt.edu.cn).

R. Liu is with the Department of Electrical and Data Engineering, University of Technology Sydney, Sydney, Australia e-mail: (renping.liu@uts.edu.au).

i.e., analyzing the impact of mobility on block propagation under a single-chain structure for the first time. Based on the dynamic equation of information propagation, the closed-form expression of single-block propagation time is derived. In addition, concerning to the forking problem that is a unique challenge in block propagation rather than the common information dissemination in a network, we characterize the blockchain forking as the multi-block competitive propagation and provide an approximate analytic solution to the multi-block competitive propagation time. The numerical and simulation results demonstrate that both the higher mobility and more moving nodes can speed up the block propagation. In addition, we also discover that distinct propagation capabilities of moving vehicles contribute to the forking reduction in the blockchain consensus.

II. Related Work

Blockchain is a revolutionary paradigm for decentralized system in that it breaks the rule that trust is commonly endorsed by an authoritative third party and realizes the direct trust establishment between nodes. In order to ensure the credibility of the on-chain information, the participators in the blockchain system need to reach a consensus by exchanging information.

In 2008, Satoshi Nakamoto first proposed the proof-of-work (PoW) algorithm in his paper to introduce Bitcoin system [12]. Due to the nature of decentralization and easy execution, PoW has become a widely accepted underlying consensus technology for digital currency applications [13]. The basic idea of PoW is a computing power competition, in which participants need to calculate the solution to a given problem but only the fastest one can win the reward. In order to reach an agreement between the distributed participators, i.e., avoiding the blockchain forking, the result is finally confirmed after six-block time (around one hour). In this way, the consensus time is unacceptable for some delay-sensitive services.

In order to tackle this issue, literature [14] proposes a Proof of Stake (PoS) mechanism, which has been applied to PPCoin (a digital currency). The basic idea is to choose the speaker via the random selection together with wealth or age of stake. According to the similar ideas, proof of X mechanisms (where X may represent identity [15], location [16], reputation [17], and so on) are proposed to replace the original time-consuming computing power competition, thereby reducing the consensus time.

In addition, Practical Byzantine Fault Tolerance (PBFT) algorithm is widely used to reach a consensus in an asynchronous environment, in which the confirmation of a new block has to be verified by at least two-thirds of the participators in the system [18]. Compared to PoW, the consensus complexity of PBFT reduces from an exponential level to a polynomial level [19]. However, the performance of PBFT drops sharply with the growing number of participating nodes due to the fact that every node needs to check with all the other nodes, which is not suitable for large-scale networks with many participating nodes [20,21]. By selecting part of vehicles as consensus nodes, a lightweight PBFT consensus protocol is designed in [22] to improve the scalability of PBFT.

In the last years, the idea of utilizing forking to speed up the consensus appears, e.g., directed acyclic graph (DAG). DAG is originally a data structure and is considered as a promising solution to dynamic programming problems (such as seeking the shortest path, topological sort, and etc.) [23]. In 2015, Sergio Demian Lerner proposed the concept of DAG-Chain, which was the first time to apply DAG into the blockchain consensus [24]. Nowadays, Tangle and Hashgraph are the two typical DAG-based consensus algorithm [25]. In Tangle, a new transaction adds to blockchain once it randomly checks two previous unconfirmed transactions [26]. One one hand, this parallel way speeds up the consensus process [27]; on the other hand, it is hard for the participators to check all transaction conflicts because a participator cannot observe the whole graph. In order to solve this problem, a coordinator mechanism is introduced to Tangle [28] but meanwhile it brings an opportunity for eavesdroppers to paralyze the entire system by attacking against the coordinator [29]. Hashgraph is an asynchronous Byzantine Fault Tolerance (BFT) algorithm [30]. In Hashgraph, each transaction is known to all nodes through the gossip protocol, and then the transactions are confirmed in sequence by a virtual voting algorithm. In this way, the confirmation delay is long at a low communication frequency.

The above mentioned studies on blockchain consensus depress the consensus time only by mechanism design. Actually, the information exchange behaviors between participators also play a significant role on the consensus. Although the communication between the participators in the blockchain system is always assumed perfect in many works [17,31,32], some investigations have realized the impact of block propagation latency on blockchain consensus failure/forking [7,33], especially in the wireless network [8,9,10]. Sun et al., find that the vulnerable wireless links in the blockchain system play an important role on the blockchain transaction transmission successful rate as well as transaction throughput and communication throughput [8]. Moreover, the signal-to-interference-plus-noise ratio (SINR), the wireless transmission power, and the number of wireless mobile miners are proved related to the performance of the wireless blockchain system [9,10]. The queueing and transmission delay under CSMA/CA also result in the longer consensus process [27], and meanwhile heavier network load brings less transactions per second (TPS) and higher transaction loss probability in wireless blockchain networks.

The impact of the imperfect information exchanges becomes stronger if the participators are moving. In the vehicular blockchain, wireless communication adopted by the moving participators limits the communication range, and meanwhile the mobility incurs the highly dynamic topologies that enables the communication more unstable. In this condition, the block forking seems more serious which further aggravates the consensus time. Literature [34] is initial to analyze the impact of node mobility on the blockchain consensus. The analytical results on the probability of adding a new block to the chain and the number of blocks exchanged during a rendezvous are derived, based on the assumption that reaching a consensus

only requires two participating nodes to confirm. In this way, the preliminary results are inappropriate to the realistic consensus process. A stability-aware consensus protocol is proposed to tackle the unstable topology problem in blockchain-based VANET but vehicles have to wait for a long period for receiving enough election messages to choose the most stable candidate [3]. Hence, few studies have an inspiriting result on characterizing the impact of the node mobility on block propagation, particularly concerning the competitions when the blockchain forking appears.

III. System Model

As is shown in Fig.1, we consider a vehicular blockchain system under the single-chain structure (e.g., PoW, PoS, etc), where every blockchain-employed vehicle (BV) is equipped with the computing, storage and wireless communication capabilities for generating, forwarding, verifying, and storing new blocks to support the blockchain protocols. No central coordinator node exists for the loyalty to the decentralization of a blockchain system.

Generally, the communications between any two vehicles adopt IEEE 802.11p or DSRC protocol [16] and the communication range of a BV is considered as a circular area. We assume that a BV moves following a random direction mobility model, and the information transmission time between two BVs is negligible relative to their rendezvous time [35,36,37]. The queuing time is also not our focus due to the fact that we analyze the block propagation in the single chain framework, where a participator transmits/chooses to forward only one same-height block, so the relationship between multiple blocks under the forking is competition instead of queueing.

In the traditional blockchain system over the wired communication, it is likely that a path always exists between any two participating nodes. In this way, it is not necessary for a participating node to forward the same block repeatedly. But in the vehicular blockchain, BV is encouraged to forward the same block repeatedly and probabilistically, where repeated forwarding is to compensate the unstable opportunistic communication caused by the mobility, and probabilistic forwarding is to utilize competition to reduce forking. A new block is added to the vehicular blockchain once the number of BVs that received and verified the block reaches a threshold. The threshold is denoted by βN, where β is in the range $(0, 1)$.

Now, we provide a new important concept— —block a holder. Block a holder is a BV that has received and verified the block a and meanwhile may forward block a to the neighboring BVs. Based on this definition, a BV may be a holder for multiple blocks.

IV. The Analysis for Block Propagation in Vehicular Blockchain Consensus

In this section, the dynamic equation of information propagation is utilized to describe the block propagation in vehicular blockchain from a macroscopic view. The analytic results on the single-block propagation time and the competitive multi-block propagation time during the consensus are derived, respectively.

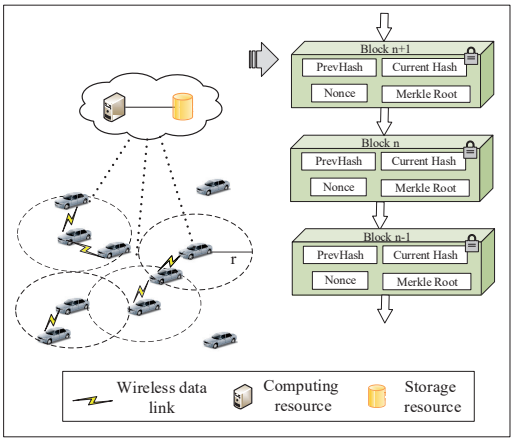

Fig. 1: Vehicular blockchain system.

A. Mapping Information Propagation Dynamic Equations into Blockchain Consensus

The dynamic equation of information propagation is originally used to portray the generation, spread and decay of a hot event in social network. It is a process in which all parties reach a unified understanding of a certain information. Analogously, the consensus in the blockchain is the collective certification for a new block by all participating nodes, which is essentially same to the formation of a social hot spot. Thus, in this paper we use the dynamic equation as a tool to analyze the propagation of a new block until it is added to the blockchain.

Considering the node mobility, we assume that the occurrences of the contacts between arbitrary two BVs follow Poisson distribution with contact rate λ [38]. When the BVs move in a random direction mobility model, the contact rate λ is given by [38]

$$\lambda \approx \frac{2rE[V^*]}{L^2} \tag{1}$$

where r is the communication range of a BV, commonly $r \ll L$. L is the side length of the area deployed vehicular blockchain. $E[V^*]$ is the average relative velocity between BVs, of which derivation is provided in Appendix.

Suppose that there are N BVs in a blockchain-based vehicular network, then a BV contacts $\lambda(N-1)$ other BVs per unit time. So, the number of BVs contacted by a BV during Δt is given by

$$m(t+\Delta t) - m(t) = \lambda(N-1)\Delta t \tag{2}$$

where $m(t)$ is the number of BVs contacted by a BV from the initial time to time t. The growth rate of the number of BVs contacted by a BV is given by

$$\frac{dm(t)}{dt} = \lambda(N-1) \tag{3}$$

B. Analysis of the Block Propagation Time during the Consensus

We consider the block propagation in vehicular blockchain as the state transitions of vehicles. In this way, we utilize

This article has been accepted for publication in a future issue of this journal, but has not been fully edited. Content may change prior to final publication. Citation information: DOI 10.1109/JIOT.2021.3074924, IEEE Internet of Things Journal

$$\begin{cases} \frac{dU_aU_b(t)}{dt} = -[I_aU_b(t) + \mu_a I_aI_b(t) + (1-\mu_a)\, I_aI_b(t) + U_aI_b(t)] * (N-1)\lambda * \frac{U_aU_b(t)}{N-1} \\ \frac{dI_aU_b(t)}{dt} = [I_aU_b(t) + \mu_a I_aI_b(t)] * (N-1)\lambda * \frac{U_aU_b(t)}{N-1} - [U_aI_b(t) + (1-\mu_a)\, I_aI_b(t)] * (N-1)\lambda * \frac{I_aU_b(t)}{N-1} \\ \frac{dU_aI_b(t)}{dt} = [U_aI_b(t) + (1-\mu_a)\, I_aI_b(t)] * (N-1)\lambda * \frac{U_aU_b(t)}{N-1} - [I_aU_b(t) + \mu_a I_aI_b(t)] * (N-1)\lambda * \frac{U_aI_b(t)}{N-1} \\ \frac{dI_aI_b(t)}{dt} = [U_aI_b(t) + (1-\mu_a)\, I_aI_b(t)] * (N-1)\lambda * \frac{I_aU_b(t)}{N-1} + [I_aU_b(t) + \mu_a I_aI_b(t)] * (N-1)\lambda * \frac{U_aI_b(t)}{N-1} \end{cases} \tag{7}$$

information propagation dynamic equations to describe the state transitions. Particularly, the consensus process of a new block commonly lasts a period, during which other same-height blocks may generate/coexist in the blockchain system, i.e., blockchain forking. As a result, a competitive relationship is formed between the coexisting blocks, which leads to the drop in the average growing rate of a block.

1) Single Block Propagation

First, we analyze the single block propagation in a non-competitive environment. The noncompetitive environment is to describe the condition that all BVs propagate the same block (e.g., block a) in a vehicular blockchain system. In this case, a BV is either in an informed state (I_a) or an uninformed state (U_a). The informed state means that the BV has received and verified block a. If a BV is in the informed state for block a, it is a block a holder. The uninformed state means that the BV has not received block a. $I_a(t)$ is the number of block a holders in time t. $U_a(t)$ is the number of BVs without block a in time t. The dynamic equation of a single block propagation is given by

$$\frac{dI_a(t)}{dt} = I_a(t) * \lambda(N-1) * \frac{U_a(t)}{N-1} \tag{4}$$

where $\frac{U_a(t)}{N-1}$ is the proportion of BVs without block a to all BVs in time t. Considering that there are $N-1$ BVs excluding the forwarding BV itself, the denominator is set to be $N-1$. If a block a holder forwards the block a to the BVs that receive it for the first time, the aggregated number of block a holders increases. Noticeably, the repeated receiving block a for a BV will not contribute to the growth of the aggregated number of block a holders.

If the initial condition $I_a(0) = 1$, the general solution to Eq.(4) is given by

$$I_a(t) = \frac{N}{1 + (N-1)e^{-\lambda N t}} \tag{5}$$

Based on the consensus mechanism in Section III, the block propagation time during the consensus process in a single-block system is given by

$$t = \frac{\ln[\frac{\beta}{1-\beta}(N-1)]}{\lambda N} \tag{6}$$

2) Multi-block Propagation

It is assumed that there are n blocks competitively spreading over a vehicular blockchain system for $n > 1$. First, we take the two-block case (e.g., block a and block b) as an example.

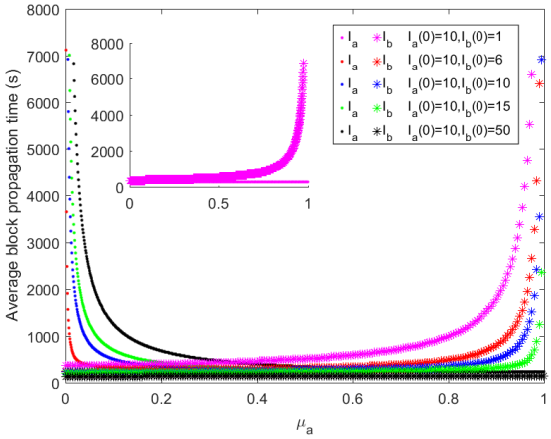

Fig. 2: The average block propagation time of block a or block b under different block forwarding possibilities μ_a in the case of two-block propagation based on the numerical solution (for $N = 300$, $r = 300m$, $\lambda = 0.222/h$, $\beta = \frac{2}{3}$).

In this condition, a BV is in one of the four possible states, i.e., uninformed of block a and uninformed of block b (denoted by U_aU_b), informed of block a but uninformed of block b (denoted by I_aU_b), uninformed of block a but informed of block b (denoted by U_aI_b), and informed of block a and informed of block b (denoted by I_aI_b). The dynamic equations of two-block propagation are given by Eq.(7).

In Eq.(7), $I_aI_b(t)$ represents the number of holders for both block a and block b in time t, $U_aU_b(t)$ represents the number of BVs without block a and block b in time t, $I_aU_b(t)$ represents the number of block a holders without block b in time t, $U_aI_b(t)$ represents the number of block b holders without block a in time t. A BV in state U_aU_b transfers to the state I_aU_b or U_aI_b once it contacts with a block holder that forwards block a or block b; a BV in state I_aU_b ($or\ U_aI_b$) transfers to the state I_aI_b once it contacts with a block holder that forwards block b ($or\ a$). In the vehicular blockchain system, a block holder selects a block that it carries to forward to its neighboring BVs. A block holder for both block a and block b forwards block a ($or\ b$) with the possibility μ_a ($or\ \mu_b = 1 - \mu_a$). In this way, the average number of BVs in state I_aI_b that forward block $a(or\ b)$ in time t is $\mu_a I_aI_b(t)$ ($or\ (1-\mu_a)I_aI_b(t)$). BVs in state I_aU_b ($or\ U_aI_b$) forward block $a(or\ b)$ in time t with the possibility 1.

Considering that $I_aI_b(t)$, $U_aI_b(t)$, $I_aU_b(t)$ and $U_aU_b(t)$ in Eq.(7) are tightly coupled, it is hard to derive the analytical solutions for $I_a(t)$ and $I_b(t)$. Thus, we provide the numerical

This article has been accepted for publication in a future issue of this journal, but has not been fully edited. Content may change prior to final publication. Citation information: DOI 10.1109/JIOT.2021.3074924, IEEE Internet of Things Journal

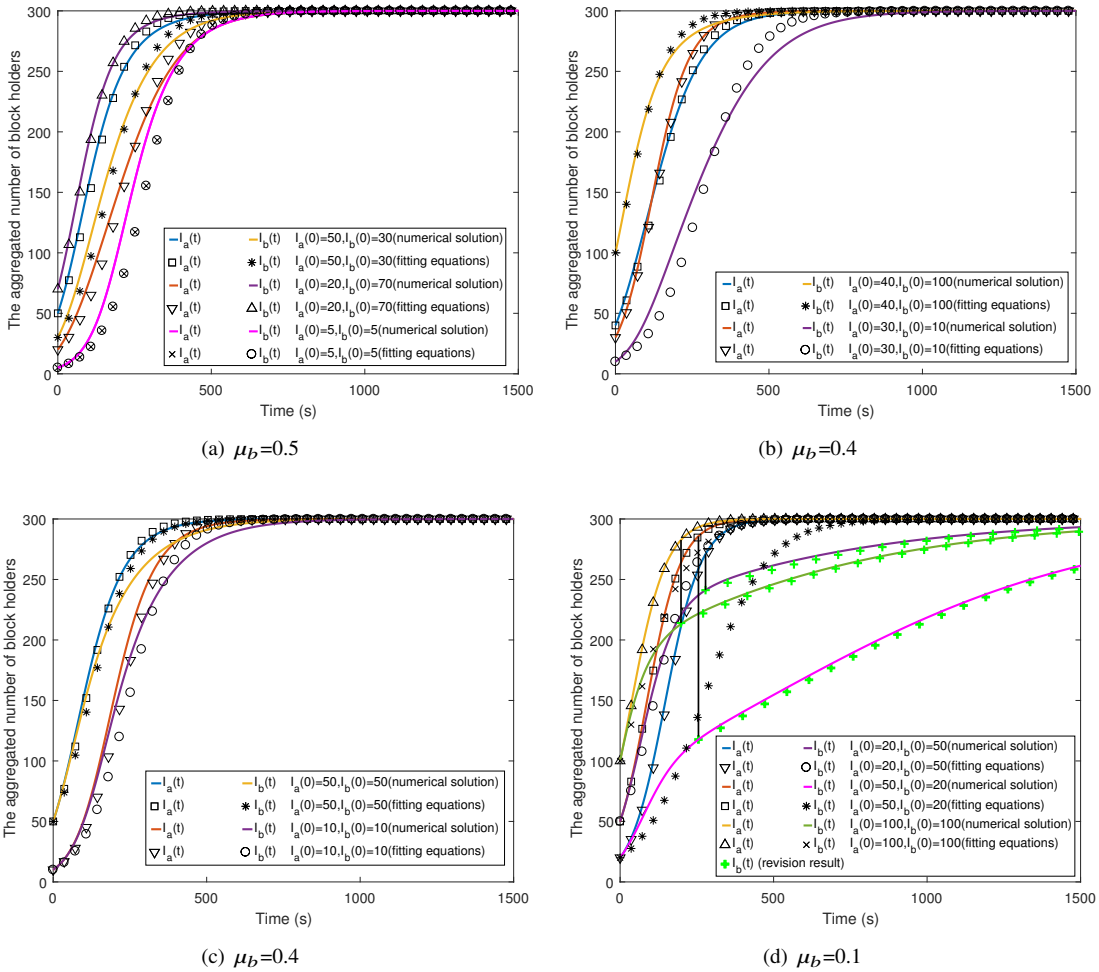

(a) μ_b=0.5 (b) μ_b=0.4

(c) μ_b=0.4 (d) μ_b=0.1

Fig. 3: The trend of the aggregated number of block a holders and block b holders over the time under different block forwarding possibilities μ_b and different initial observed conditions in the case of two-block propagation based on the numerical solution and fitting equations ($N = 300$, $r = 300m$, $\lambda = 0.222/h$).

solution to Eq.(7) by using ode45 in MATLAB [39] and plot the curves of the aggregated number of block holders. Fig.2 provides the block propagation time of a two-block competitive propagation. We can easily find that the block propagation time of block a descends as μ_a increases (equivalently, μ_b decreases). Meanwhile, the initial number of a block (i.e., $I_a(0)$ or $I_b(0)$) affects the propagation time of other blocks. The minimum average block propagation time for a block appears in $\mu_a = \mu_b = 1/2$ for $I_a(0) = I_b(0)$. The minimum average block propagation time for a block appears in $0.5 < \mu_a < 1$ (equivalently, $0 < \mu_b < 0.5$) for $I_a(0) < I_b(0)$. Contrarily, the minimum average block propagation time for a block appears in $0 < \mu_a < 0.5$ (equivalently, $0.5 < \mu_b < 1$) for $I_a(0) > I_b(0)$. Thus, assigning lower forwarding probability to the block with high initial block holders and assigning higher forwarding probability to the block with low initial block holders can decrease the average block propagation time.

Based on the varying trend of Eq.(5) over the time and the equation of $I_a(t)$ $(or\ I_b(t)$ at a particular μ_a $(or\ \mu_b)$, together with a conclusion from Fig.2 that the initial number of a block (i.e., $I_a(0)$ or $I_b(0)$) affects the propagation time of other blocks, we further provide the fitting equations for $I_a(t)$ and $I_b(t)$. The fitting equation to $I_b(t)$ is given by

$$I_b(t) = \frac{N}{1 + (\frac{N}{I_b(0)} - 1)e^{-\lambda N t * e^{-(1-\mu_b)\frac{I_a(0)}{I_a(0)+I_b(0)}}}} \tag{8}$$

The fitting equation degenerates to Eq.(5) for $\mu_b = 1$, i.e., the single-block propagation equation. Based on the consensus mechanism in Section III, the block propagation time during the consensus process in a two-block system is given by

$$t_b = \frac{\ln[\frac{\beta}{1-\beta}(\frac{N}{I_b(0)} - 1)]}{\lambda N} * e^{(1-\mu_b)\frac{I_a(0)}{I_a(0)+I_b(0)}} \tag{9}$$

Analogously, we can derive the fitting expression for the propagation time of block a holders.

Fig.3 depicts the trend of the aggregated number of block a holders and block b holders over the time under different propagation capabilities involving block forwarding possibilities and different initial number of block holders. The conditions in Fig.3 can be divided into two classifications,

This article has been accepted for publication in a future issue of this journal, but has not been fully edited. Content may change prior to final publication. Citation information: DOI 10.1109/JIOT.2021.3074924, IEEE Internet of Things Journal

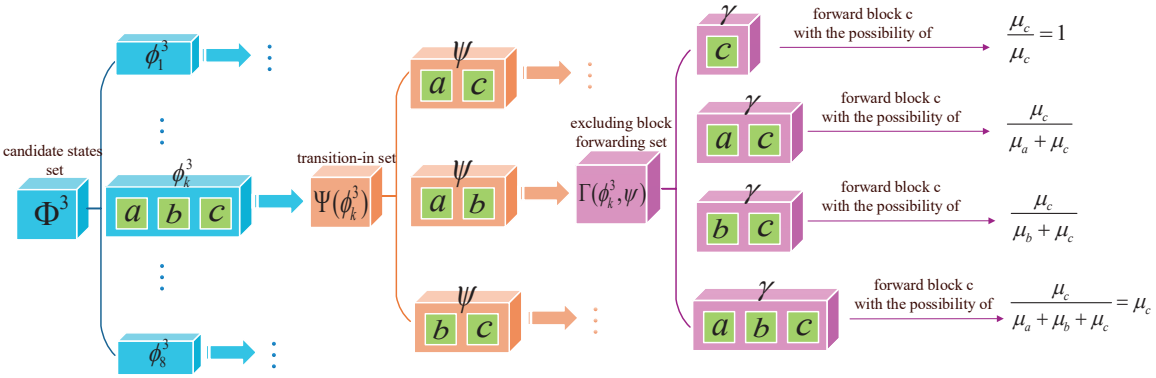

Fig. 4: An example of three-block competitive propagation.

$$\frac{d\phi_k^n(t)}{dt} = \sum_{\psi\in\Psi\left(\phi_k^n\right)}\left\{\left[\sum_{\gamma\in\Gamma\left(\phi_k^n,\psi\right)}\frac{\sum_{x\in\left(\phi_k^n-\psi\right)}\mu_x}{\sum_{x\in\gamma}\mu_x}\gamma(t)\right]*\lambda(N-1)*\frac{\psi(t)}{N-1}\right\} - \left[\sum_{\phi_j^n\in\Phi^n}\frac{\sum_{x\in\left(\phi_j^n-\phi_k^n\right)}\mu_x}{\sum_{x\in\phi_j^n}\mu_x}\phi_j^n(t)\right]*\lambda(N-1)*\frac{\phi_k^n(t)}{N-1} \tag{11}$$

i.e., the well-matched competition and the mismatched competition. The well-matched competition means the similar propagation capabilities for different blocks, that depends on their forwarding probabilities and initial number of blocks. While, the mismatched competition means a great disparity in propagation capability for different blocks.

- Well-matched competition: We observe a good matching between the numerical results and the fitting results to $I_a(t)$ and $I_b(t)$ when the forwarding probabilities of block a and block b are approximate regardless of the initial number of block holders, as is shown in Fig.3(a), (b) and (c). Especially, the perfect matching appears in the condition that μ_a is equal to μ_b.
- Mismatched competition: As Fig.3(d) show, Eq.(8) fits well with the numerical results of the aggregated number of block a if the forwarding probability μ_a is far larger than μ_b, but contrarily, it leads a poor fitting to block b. More specifically, we find that the deviation from the fitting result to $I_b(t)$ appears at the back of the curve. The reason is that the block propagation seems degenerating to the single-block propagation (i.e., block b propagation) once block a has propagated to nearly all BVs. For example, the deviation appears when $I_a(t)$ reaches 280 (out of 300), 285 (out of 300) and 275 (out of 300), as is shown in Fig.3(d). In this condition, the two-block system can be approximately regarded as a single block system but each BV forwards block b with the possibility μ_b. In this way, Eq.(8) is corrected by

$$I_b(t) = \frac{N}{1+\left(\frac{N}{I_b(t_1)}-1\right)e^{-\lambda N(t-t_1)\mu_b}} \quad (t\geq t_1) \tag{10}$$

where t_1 is the time when the deviation appears, that equals to the time when most of the BVs have received the block with strong propagation capability. In this case, t_1 is calculated by Eq.(7) for $I_a(t) = 0.9N$.

Hence, the forwarding probability plays a overwhelming role on the fitting results. The good fitting happens as long as the forwarding probability is well-matched for all blocks or is for the block with higher forwarding probability under the mismatched competition condition. For the block with weak propagation capability, the fitting equation is corrected by Eq.(10).

Now, we discuss the n-block propagation in a competitive environment for $n > 1$. The state of a BV is described by the set of the blocks carried by it. In this way, the number of candidate states for a BV is 2^n. A general dynamic equation for n-block competitive propagation is given by Eq.(11).

The explanations of the parameters in Eq.(11) are listed in the following.

- Candidate states set Φ^n: $\Phi^n = \{\phi_k^n \,|1\leq k\leq 2^n\,, k\in Z\}$ is a set of candidate states for a BV in an n-block system, where ϕ_k^n is the k-th state, and $\phi_k^n(t)$ represents the number of BVs in state ϕ_k^n in time t.
- Transition-in set $\Psi\left(\phi_k^n\right)$: $\Psi\left(\phi_k^n\right) = \{\psi|\ \psi\subset\phi_k^n, |\psi| = \left|\phi_k^n\right|-1\}$ is a set of states with $\left|\phi_k^n\right|-1$ blocks, where ψ is one of the states, and $\psi(t)$ represents the number of BVs in state ψ in time t. Since the states of $\left|\phi_k^n\right|-1$ blocks that belong to state ϕ_k^n could transfer to state ϕ_k^n, a BV in state ψ transfers to the state ϕ_k^n once it contacts with a block holder forwarding the block $\phi_k^n-\psi$.
- Excluding block forwarding set $\Gamma\left(\phi_k^n,\psi\right)$: $\Gamma\left(\phi_k^n,\psi\right) = \{\gamma\,|\gamma\in\Phi^n, \left(\phi_k^n-\psi\right)\subseteq\gamma\}$ is a set of states with the block that belongs to $\phi_k^n-\psi$, where γ is one of the states, and $\gamma(t)$ represents the number of BVs in state γ in time t. It is worth noting that there is only one block in state $\phi_k^n-\psi$.

The first term in Eq.(11) describes the growth of the number of BVs in state ϕ_k^n. The second term considers the descent of the number of BVs in state ϕ_k^n because a BV in state ϕ_k^n transfers to another state once it contacts with a block holder

This article has been accepted for publication in a future issue of this journal, but has not been fully edited. Content may change prior to final publication. Citation information: DOI 10.1109/JIOT.2021.3074924, IEEE Internet of Things Journal

forwarding the block not in ϕ_k^n in time t.

A holder with n blocks, forwards block x with the possibility μ_x. The sum of these block forwarding probabilities equal one, i.e., $\sum_x \mu_x = 1$. It is worth noting that a BV has no idea of the coexisting blocks in the system at a time, but it knows the blocks that it has received. So, a BV in state γ forwards the block that belongs to $\phi_k^n - \psi$ with the possibility $\frac{\sum_{x\in(\phi_k^n-\psi)}\mu_x}{\sum_{x\in\gamma}\mu_x}$, where $\sum_{x\in\gamma}\mu_x$ represents the sum of forwarding possibility of all blocks belonging to γ. A BV in state ϕ_j^n forwards the block without in ϕ_k^n with the possibility $\frac{\sum_{x\in(\phi_j^n-\phi_k^n)}\mu_x}{\sum_{x\in\phi_j^n}\mu_x}$.

Now, we provide an example of three-block competitive propagation shown in Fig.4. Let ϕ_k^3 is $\{a,b,c\}$ in the three-block case (e.g., block a, block b and block c) where their forwarding probabilities are μ_a, μ_b and μ_c for $\mu_a+\mu_b+\mu_c=1$. In this case, the transition-in set is $\Psi\left(\phi_k^3\right)=\{\psi\,|\psi=\{a,b\}\,or\,\psi=\{a,c\}\,or\,\psi=\{b,c\}\}$. Then, we choose $\psi=\{a,b\}$ for an instance. The excluding block is block c and the corresponding forwarding set is $\Gamma\left(\phi_k^3,\psi\right)=\{\gamma\,|\gamma=\{c\}\,or\,\gamma=\{a,c\}\,or\,\gamma=\{b,c\}\,or\,\gamma=\{a,b,c\}\}$. The forwarding probabilities of block c in different state γ are shown in Fig.4, where a block holder of block a, b and c forwards block c with the possibility μ_c; a block holder of block b and c forwards block c with the possibility $\frac{\mu_c}{\mu_b+\mu_c}$; a block holder of block a and block c forwards block c with the possibility $\frac{\mu_c}{\mu_a+\mu_c}$; a block holder of block c forwards block c with the possibility 1.

Our analysis method is always correct for some other moving models, e.g., random waypoint mobility model, random direction mobility model and even the real trace based vehicle mobility model. The reason is that different moving models only affect the contact rate of BVs in the dynamic equations of block propagation. For example, the contact rate of random waypoint mobility model is $\lambda_{RWP}\approx\frac{2\omega rE[V^*]}{L^2}$, and the contact rate of random direction model is $\lambda_{RD}\approx\frac{2rE[V^*]}{L^2}$. As long as λ is given, we can use the proposed method to analyze the block propagation under different moving models.

V. Simulation and Discussion

In this section, we evaluate the aggregated number of block holders or the block propagation time during the consensus in vehicular blockchain. First, we compare the numerical results and the simulation results to prove the validity of the theoretical analysis. Meanwhile, the results show the impacts of the communication range, velocity of BVs, the number of BVs and the network coverage on the block propagation time. Finally, the impact of the mismatched propagation capabilities of BVs on forking is shown.

A. Scenario Description

We consider a $12km*12km$ square region in which 100~1000 BVs move in a random direction mobility model. Specifically, the velocity follows the uniform distribution with the lower bound $20km/h$ and the upper bound $60km/h$, which are within the range of the normal vehicle moving speed. The moving direction follows the uniform distribution in $[0,2\pi)$. The communication range of a BV is from 70m to 300m [40]. The contact rate λ depends on the area of the whole region, the communication range of a BV, and the average relative velocity between BVs [41]. Eq.(1) provides the way to calculate the value of λ under random direction model. For example, in a $12km*12km$ region,

- λ is $0.0518/h$ when the communication range is 70m and the velocity of BVs follows the uniform distribution with the lower bound $20km/h$ and the upper bound $60km/h$.
- λ is $0.074/h$ when the communication range is 100m and the velocity of BVs follows the uniform distribution with the lower bound $20km/h$ and the upper bound $60km/h$.
- λ is $0.148/h$ when the communication range is 200m and the velocity of BVs follows the uniform distribution with the lower bound $20km/h$ and the upper bound $60km/h$.
- λ is $0.222/h$ when the communication range is 300m and the velocity of BVs follows the uniform distribution with the lower bound $20km/h$ and the upper bound $60km/h$.

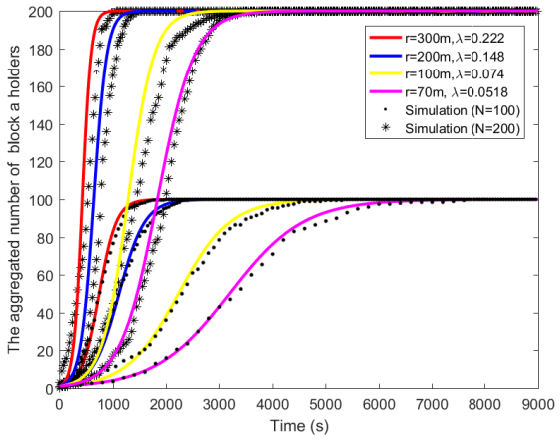

Fig. 5: The aggregated number of block holders in one-block condition over the time in a $12km*12km$ square region ($N=100$ and $N=200$).

Recalling the assumption that a new block is added to the vehicular blockchain once the number of BVs that received and verified the block reaches a threshold βN, we take $\beta=2/3$ as an example. Of course, we may adopt other threshold values (such as β =3/4, 4/5, etc.), as long as it satisfies the idea of blockchain, i.e., following the most participators.

In the following subsections, the numerical results are the solution to the dynamic equations of block propagation calculated by ode45 in MATLAB, while the simulation results are averaged over 1000 simulation rounds.

B. Results Discussion

Fig.5 depicts the aggregated number of block holders over the time in the condition that all BVs propagate the same block. We observe a good matching between the numerical results (represented by solid lines) and the simulation results (represented by dots). Initially, the aggregated number of block holders grows with time, but the growth rate descends when the majority of BVs have received it due to the saturation for

This article has been accepted for publication in a future issue of this journal, but has not been fully edited. Content may change prior to final publication. Citation information: DOI 10.1109/JIOT.2021.3074924, IEEE Internet of Things Journal

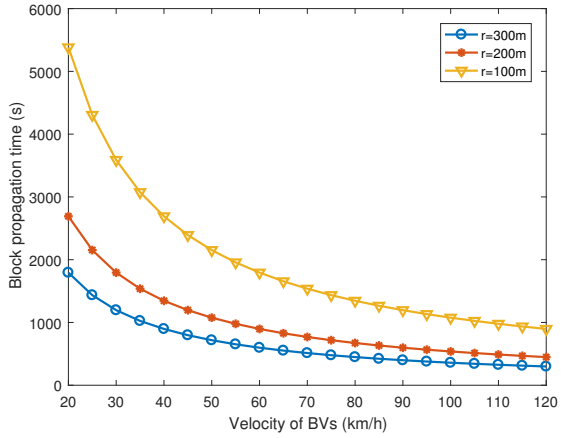

Fig. 6: The influence of the velocity of BVs on the block propagation time in a $12km * 12km$ square region ($N = 100$, $r = 100m, 200m, 300m$, $\beta = \frac{2}{3}$).

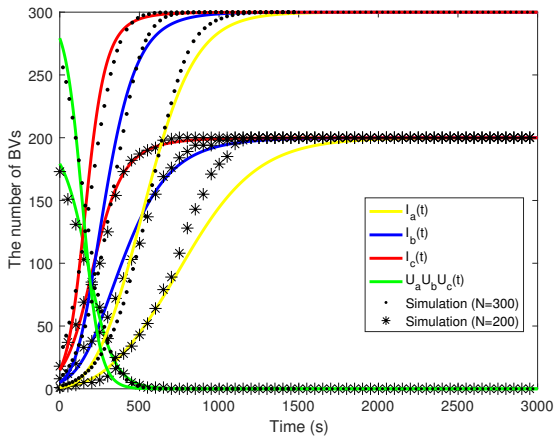

Fig. 8: The number of BVs in different states over time in the case of three-block propagation in a $12km * 12km$ square region ($N = 200$ and $N = 300$, $r = 300m$, $\lambda = 0.222/h$).

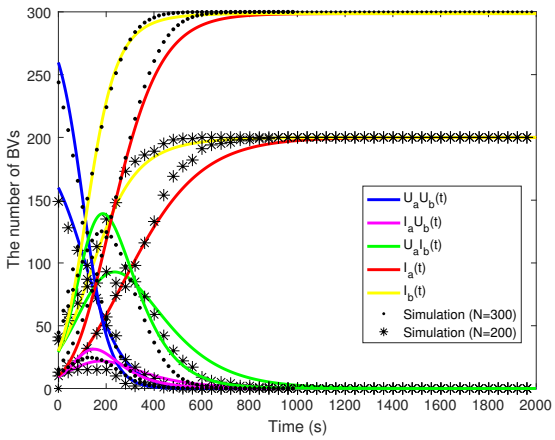

Fig. 7: The number of BVs in different states over time in the case of two-block propagation in a $12km * 12km$ square region ($N = 200$ and $N = 300$, $r = 300m$, $\lambda = 0.222/h$).

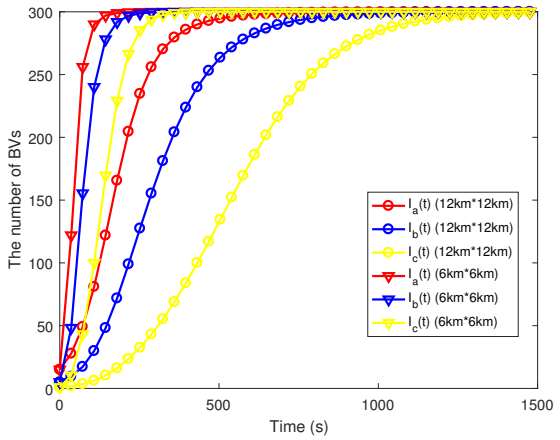

Fig. 9: The number of BVs in different states over time in the case of three-block propagation in a $12km * 12km$ square region and $6km * 6km$ square region ($N = 300$, $r = 300m$, $\lambda = 0.222/h$ and $\lambda = 0.8884/h$).

the same block from the past. The growth slope is mainly determined by the contact rate λ which is $0.0518/h$, $0.074/h$, $0.148/h$ and $0.222/h$ from the communication range 70m, 100m, 200m and 300m. Thus, we can find that a larger communication range yields a greater λ that further brings a faster block propagation. In addition, the comparison of different BVs agrees with our intuition of shorter propagation time under higher BV density. For example, the pink lines ($r = 70m$) in Fig.5 say that the propagation completion of 200 BVs appears earlier than that of 100 BVs.

Fig.6 shows the negative correlation between the velocity of BVs and the block propagation time, which indicates an inspiring result that mobility speeds up the block propagation. The reason is that a faster velocity yields a greater λ that further speeds up block propagation. Meanwhile, we can find that the impact of communication range is crippled by the velocity of BVs.

Fig.7 and Fig.8 show the number of BVs under the different states in a two-block (i.e., block a and block b) and a three-block (e.g., block a, block b and block c) system, respectively. In Fig.7, the forwarding probability for any block in the two-block case is $1/2$ and the initial observed conditions are $I_a(0) = 10$ and $I_b(0) = 30$. Over the time, the number of BVs in state U_aU_b descends to the zero, and contrarily, the number of BVs with block a or block b (i.e. $I_a(t)$ and $I_b(t)$) lasts growing until to the condition that all BVs have received the block. The number of BVs in state U_aI_b (or I_aU_b) is a hill-shape curve over the time. The lower peak of I_aU_b than that of U_aI_b is because the less block a holders than block b holders in the initial time. Analogously, the results of three-block case are provided in Fig.8 where the forwarding probability for any block is $1/3$ and the initial observed conditions are $I_a(0) = 1$, $I_b(0) = 5$ and $I_c(0) = 15$.

The comparison of different network coverage in Fig.9 agrees with our intuition of shorter propagation time under higher BV density and greater λ. For example, the red lines in Fig.9 say that the propagation completion of BVs in a $6km * 6km$ square region appears earlier than that of BVs in a $12km * 12km$ square region.

Fig.10 illustrates the impact of the number of BVs on the average block propagation time in the single-block and

This article has been accepted for publication in a future issue of this journal, but has not been fully edited. Content may change prior to final publication. Citation information: DOI 10.1109/JIOT.2021.3074924, IEEE Internet of Things Journal

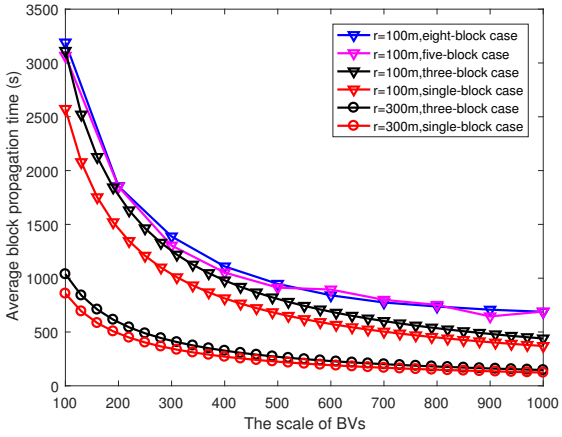

Fig. 10: The influence of the scale of BVs on the average block propagation time in single-block and multi-block condition over a $12km * 12km$ square region ($N = 100 \sim 1000$, $\beta = \frac{2}{3}$).

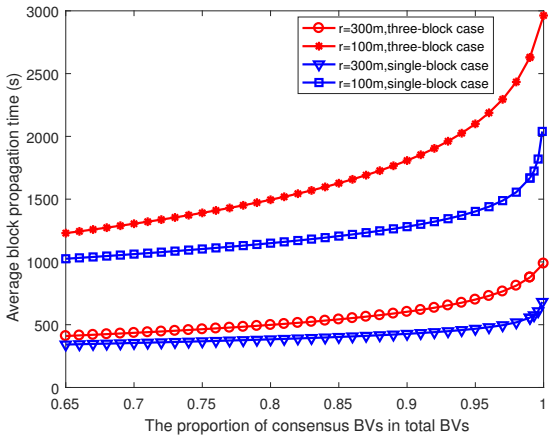

Fig. 11: The relationship between the threshold and the average block propagation time in the case of single-block propagation where the initial condition is $I_a(0) = 1$ and in the case of three-block propagation where the forwarding probability for any block is $1/3$ and the initial conditions are $I_a(0) = 1$, $I_b(0) = 1$ and $I_c(0) = 1$ based on the numerical solution in a $12km * 12km$ square region ($N = 300$).

multi-block condition. The propagation competitions between multiple blocks play a smaller role on the large-scale BV scenario than on the small-scale BV scenario. An interesting result shown in Fig.10 is that more BVs result in a faster block propagation. The reason is that the time shown in Eq.(6) (i.e., $t = \frac{\ln[\frac{\beta}{1-\beta}(N-1)]}{\lambda N}$) is decreasing with N. Meanwhile, we can easily find that the impact of communication range is crippled by the denser BVs. In addition, more competitive propagation blocks lead to longer block propagation time.

In this paper, we assume that a new block is added to the vehicular blockchain once the number of BVs that received and verified the block reaches a threshold. Fig.11 shows that growth of the average block propagation time seems in an exponential way with the increasing threshold. That indicates that the fully propagation is much more difficult than that of almost propagation. For example, the average block propagation time is around 2100s for 285 BVs but reaches to 3000s for 300 BVs in the three-block case. Hence, the almost propagation is potential on the propagation time reduction, which is consistent with the results about the fully connectivity and almost connectivity in random network [42].

Based on the previous simulations, we prove the initial impact of propagation capabilities of BVs (including the forwarding probability and the initial number of a block) on the block propagation. Now, we characterize the forking by incorporating multi-block competitive forwarding at each participator. The forwarding probability of a BV to transmit block a depends on the state of all received same-height blocks and the ratio of the number of receiving block a to all received same-height blocks so far. In this way, a BV prefers to transmit the most received block based on its own observation, which widens the gap between different blocks. Thus, the forking is restrained through controlling the propagation capability.

Fig.12 illustrates the impact of propagation capability on the block propagation time, comparing to the minimum block propagation time. Here, the minimum block propagation time, that is proved in Fig.2, is regarded as a performance benchmark. A BV prefers to transmit the most received block

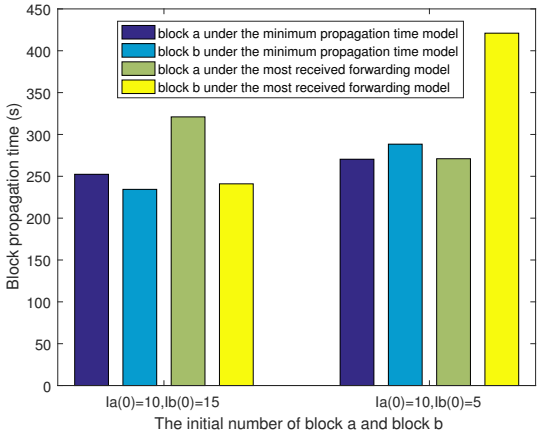

Fig. 12: The average block propagation time of block a and block b under the most received forwarding model and the minimum propagation time model.

based on its own observation, which is in favor of widening the gap of propagation capabilities between different blocks. From Fig.12, we discover that the propagation time of the block with the strong propagation capability approximates to the minimum block propagation time. Moreover, the wide gap appears between block a and block b. For example, the propagation time of block b approximates to the minimum block propagation time in the left group. In this group, block b is of the strong propagation capability, since its initial value $I_b(0)$ is larger than $I_a(0)$, thereby further incurring the higher forwarding probability for block b. Similarly, the right group also provides the same conclusion. The gap of the block propagation time between the block a and block b shown in Fig.12 implies forking reduction. Thus, the forking is depressed through controlling the propagation capability.

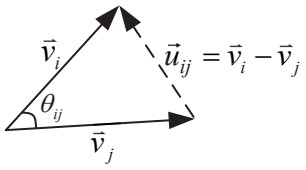

Fig. 13: Vector illustration of relative velocity between two BVs.

VI. Conclusion

In this paper, we investigate the impact of mobility on block propagation during the consensus in vehicular blockchain. Based on the dynamic equation of information propagation, the closed-form expression of single-block propagation time is derived. In addition, we characterize the blockchain forking as the multi-block competitive propagation and provide an approximate analytic solution to the multi-block competitive propagation time. The numerical and simulation results demonstrate that both the higher mobility and more moving nodes can speed up the block propagation, and the mismatched propagation capabilities of moving vehicles are in favor of the forking reduction in the blockchain consensus.

Appendix

In this section, we derive the closed-form expression of $E[V^*]$ in detail. Based on the assumption in Section III that a BV moves following the random direction mobility model, a BV is randomly assigned an initial velocity v, a finite movement duration σ, and a movement direction θ. The velocity v follows the uniform distribution of $[V_{\min}, V_{\max}]$, and the angle θ follows the uniform distribution of $[0, 2\pi)$. If a BV reaches to the boundary of the area, it will continue to move to the symmetric boundary with the same velocity and direction.

The velocity of the i-th BV is a 3-tuple vector, denoted by $\vec{v}_i = \{v_i, \theta_i, \sigma_i\}$. The relative velocity between the i-th BV and the j-th BV is shown in Fig.13, of which module value is given by

$$\begin{aligned}\left|\vec{u}_{ij}\right| &= \sqrt{(\vec{v}_i - \vec{v}_j)\cdot(\vec{v}_i - \vec{v}_j)} \\ &= \sqrt{\vec{v}_i\cdot\vec{v}_i - 2\vec{v}_i\cdot\vec{v}_j + \vec{v}_j\cdot\vec{v}_j}\end{aligned} \tag{12}$$

As shown in Fig.13, the angle between the moving direction of the i-th BV and that of the j-th BV is θ_{ij}. It follows the uniform distribution of $[0, 2\pi)$.

(1) for $V_{\min} = V_{\max} = v$, $E[V^*]$ is given by

$$\begin{aligned}E[V^*] &= \frac{1}{2\pi}\int_0^{2\pi}\left|\vec{u}_{ij}\right| d\theta_{ij} \\ &= \frac{1}{2\pi}\int_0^{2\pi}\sqrt{2v^2 - 2v^2\cos\theta_{ij}}\, d\theta_{ij} \\ &= \frac{4v}{\pi}\end{aligned} \tag{13}$$

On this basis, Eq.(1) is rewritten as

$$\lambda \approx \frac{8rv}{\pi L^2} \tag{14}$$

(2) for $V_{\min} \neq V_{\max}$, $E[V^*]$ is given by

$$E[V^*] = \frac{1}{\pi(v_i - v_j)^2}\int_0^{\pi}\int_{V_{\min}}^{V_{\max}}\int_{V_{\min}}^{V_{\max}}\sqrt{v_i^2 + v_j^2 - 2v_i v_j\cos\theta_{ij}}\, dv_i dv_j d\theta_{ij} \tag{15}$$

Acknowledgment

The work was supported by the National Natural Science Foundation of China (Grant No. 61941114, 61701037), the National High Technology Research and Development of China (2014AA01A701) and National Youth Top-notch Talent Support Program.

References

[1] M. B. Mollah, J. Zhao, D. Niyato, et al, Blockchain for the Internet of Vehicles towards Intelligent Transportation Systems: A Survey, *IEEE Internet of Things Journal*, vol. 8, no. 6, 2020, pp. 4157-4185.

[2] Y. Lu, X. Huang, Y. Dai, et al, Blockchain and Federated Learning for Privacy-Preserved Data Sharing in Industrial IoT, *IEEE Transactions on Industrial Informatics*, vol. 16, no. 6, 2020, pp. 4177-4186.

[3] Z. Jiao, B. Zhang, L. Zhang, et al, A Blockchain Based Computing Architecture for Mobile Ad-Hoc Cloud, *IEEE Network*, vol. 34, no. 4, 2020, pp. 140-149.

[4] T. Li, N. N. Xiong, J. Gao, Reliable Code Disseminations Through Opportunistic Communication in Vehicular Wireless Networks, *IEEE Access*, vol. 6, 2018, pp. 55509-55527.

[5] Y. Xiao, N. Zhang, W. Lou, et al, A Survey of Distributed Consensus Protocols for Blockchain Networks, *IEEE Communications Surveys & Tutorials*, vol. 22, no. 2, 2020, pp. 1432-1465.

[6] Y. Li, B. Cao, M. Peng, L. Zhang, D. Feng and J. Yu, Direct Acyclic Graph-based Ledger for Internet of Things: Performance and Security Analysis, *IEEE/ACM Transactions on Networking*, vol. 28, no. 4, pp. 1643-1656, Aug. 2020.

[7] L. Wan, D. Eyers and H. Zhang, Evaluating the Impact of Network Latency on the Safety of Blockchain Transactions, *2019 IEEE International Conference on Blockchain (Blockchain)* IEEE, 2019, pp. 194-201.

[8] Y. Sun, L. Zhang, G. Feng, et al, Blockchain-enabled wireless Internet of Things: Performance analysis and optimal communication node deployment, *IEEE Internet of Things Journal*, vol.6, no. 3, 2019, pp. 5791-5802.

[9] H. Xu, L. Zhang, Y. Liu and B. Cao, RAFT Based Wireless Blockchain Networks in the Presence of Malicious Jamming, *IEEE Wireless Communications Letters*, vol. 9, no. 6, 2020, pp. 817-821.

[10] G. Lee, J. Park, W. Saad, et al, Performance Analysis of Blockchain Systems With Wireless Mobile Miners, *IEEE Networking Letters*, vol. 2, no. 3, 2020, pp. 111-115.

[11] Z. Zheng, J. Pan, and L. Cai, Lightweight Blockchain Consensus Protocols for Vehicular Social Networks, *IEEE Transactions on Vehicular Technology*, vol. 69, no. 6, 2020, pp. 5736-5748.

[12] S. Nakamoto, Bitcoin: A Peer-to-Peer Electronic Cash System, 2008, pp. 1-9. Available: http://bitcoin.org/bitcoin.pdf.

[13] R. Grinberg, Bitcoin: An Innovative Alternative Digital Currency, *Hastings Science & Technology Law Journal*, vol. 4, 2011, pp. 1-50.

[14] S. King, S. Nadal, PPCoin: Peer-to-Peer Crypto-Currency with Proof-of-Stake, 2012, pp. 1-6.

[15] S. De Angelis, L. Aniello, R. Baldoni, et al., PBFT vs Proof-of-authority: Applying the CAP Theorem to Permissioned Blockchain, *2nd Italian Conference on Cyber Security*, Milan, Italy, 2018, pp. 1-11.

[16] M. Amoretti, G. Brambilla, F. Medioli and F. Zanichelli, Blockchain-Based Proof of Location, *2018 IEEE International Conference on Software Quality, Reliability and Security Companion (QRS-C)*, Lisbon, Portugal, 2018, pp. 146-153.

[17] J. Kang et al., Blockchain for Secure and Efficient Data Sharing in Vehicular Edge Computing and Networks, *IEEE Internet of Things Journal*, vol. 6, no. 3, 2019, pp. 4660-4670.

[18] A. Miller, Y. Xia, K. Croman, et al., The Honey Badger of BFT Protocols, *2016 ACM SIGSAC Conference on Computer and Communications Security*, Vienna, Austria, 2016, pp. 31-42.

[19] H. Sukhwani, J. M. Mart ´ı nez, et al., Performance Modeling of PBFT Consensus Process for Permissioned Blockchain Network (Hyperledger Fabric), *2017 IEEE 36th Symposium on Reliable Distributed Systems (SRDS)*, Hong Kong, China, 2017, pp. 253-255.

[20] M. Du, X. Ma, et al., A Review on Consensus Algorithm of Blockchain, *2017 IEEE International Conference on Systems, Man, and Cybernetics (SMC)*, Banff, Canada, 2017, pp. 2567-2572.

[21] X. Zhang, J. Liu, Y. Li, et al., Blockchain Based Secure Package Delivery via Ridesharing, *2019 11th International Conference on Wireless Communications and Signal Processing (WCSP)*, Xi' an, China, 2019, pp. 1-6.

[22] S. Kudva, S. Badsha, S. Sengupta, et al, Towards Secure and Practical Consensus for Blockchain based VANET, *Information ences*, vol. 545, 2020.

[23] B. Shipley, A New Inferential Test for Path Models Based on Directed Acyclic Graphs, *Structural Equation Modeling*, vol. 7, no. 2, 2000, pp. 206-218.

[24] S. D. Lerner, DagCoin draft, 2015. [Online]. Available: https://bitslog.files.wordpress.com/2015/09/dagcoin-v41.pdf.

[25] B. Cao, et al., When Internet of Things Meets Blockchain: Challenges in Distributed Consensus, *IEEE Network*, vol. 33, no. 6, 2019, pp. 133-139.

[26] S. Popov, The Tangle (Version 1.4.3), 2018, pp.1-28.

[27] B. Cao, M. Li, L. Zhang, et al., How Does CSMA/CA Affect the Performance and Security in Wireless Blockchain Networks, *IEEE Transactions on Industrial Informatics*, vol. 16, no. 6, 2020, pp. 4270-4280.

[28] Q. Bramas, The Stability and the Security of the Tangle, 2018.

[29] B. C. Florea, Blockchain and Internet of Things data provider for smart applications, *2018 7th Mediterranean Conference on Embedded Computing (MECO)*, Budva, Montenegro, 2018, pp. 1-4.

[30] L. Zhao, J. Yu, Evaluating DAG-Based Blockchains for IoT, *2019 18th IEEE International Conference On Trust, Security And Privacy In Computing And Communications/13th IEEE International Conference On Big Data Science And Engineering (TrustCom/BigDataSE)* IEEE, 2019, pp. 507-513.

[31] L. Xie, Y. Ding, H. Yang, et al, Blockchain-based Secure and Trustworthy Internet of Things in SDN-Enabled 5G-VANETs, *IEEE Access*, vol .7, 2019, pp. 56656-56666.

[32] J. Kang, Z. Xiong, D. Niyato, et al, Toward Secure Blockchain-Enabled Internet of Vehicles: Optimizing Consensus Management Using Reputation and Contract Theory, *IEEE TRANSACTIONS ON VEHICULAR TECHNOLOGY*, vol. 68, no. 3, 2019, pp. 2906-2920.

[33] C. Decker, R. Wattenhofer, Information propagation in the Bitcoin network, *IEEE P2P 2013 Proceedings* IEEE, 2013, pp. 1-10.

[34] S. Kim, Impacts of Mobility on Performance of Blockchain in VANET, *IEEE Access*, vol. 7, 2019, pp. 68646-68655.

[35] M. Khabbaz, Modelling and Analysis of a Novel Vehicular Mobility Management Scheme to Enhance Connectivity in Vehicular Environments, *IEEE Access*, vol. 7, 2019, pp. 120282-120296.

[36] C. Celes, F. A. Silva, A. Boukerche, et al, Improving Delay and Energy Efficiency of Vehicular Networks Using Mobile Femto Access Points, *IEEE Transactions on Mobile Computing*, vol. 16, no. 12, 2017, pp. 3376-3389.

[37] J. Chen, G. Mao, C. Li, Capacity of Cooperative Vehicular Networks With Infrastructure Support: Multiuser Case, *IEEE Transactions on Vehicular Technology*, vol. 67, no. 2, 2018, pp. 1546-1560.

[38] X. Zhang, G. Neglia, J. Kurose, et al., Performance modeling of epidemic routing, *NETWORKING 2006, Networking Technologies, Services, and Protocols; Performance of Computer and Communication Networks; Mobile and Wireless Communications Systems*, Springer Berlin Heidelberg, vol. 51, 2006, pp. 827-839.

[39] L. F. SHAMPINE, M. W. REICHELT, The MATLAB ODE Suite, *Society for Industrial and Applied Mathematics*, vol. 18, 1997, pp. 1-22.

[40] X. Zhang; X. Chen, Data Security Sharing and Storage Based on a Consortium Blockchain in a Vehicular Ad-hoc Network, *IEEE Access*, vol. 7, 2019, pp. 58241-58254.

[41] T. Ghandriz, B. Jacobson, P. Nilsson, et al, Computationally Efficient Nonlinear One- and Two-Track Models for Multitrailer Road Vehicles, *IEEE Access*, vol. 8, 2020, pp. 203854-203875.

[42] M. Franceschetti, R. Meester, Random Networks for Communication (From Statistical Physics to Information Systems), 2008.

Xuefei Zhang (Member, IEEE) received the B.S. and Ph.D. degrees in telecommunications engineering from the Beijing University of Posts and Telecommunications (BUPT) in 2010 and 2015, respectively. From September 2013 to August 2014, she was visiting the School of Electrical and Information Engineering, University of Sydney, Australia. She is currently with the National Engineering Lab, BUPT. Her research area includes mobile edge computing, blockchain, reinforcement learning and intelligent transportation system.

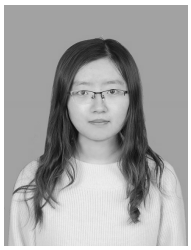

Wenbo Xia received her B.S. degree in communication engineering from Beijing University of Posts and Telecommunications (BUPT), Beijing, China, in 2020. She is currently pursuing the M.S. degree in Electrical and Information Engineering with the Beijing University of Posts and Telecommunications. Her current research interests mainly focus on blockchain in vehicular networks.

Xiaochen Wang received the Ph.D. degree in system science from Beijing University of Posts and Telecommunications (BUPT), Beijing, China, in 2019. She is currently a postdoctor of the National Engineering Laboratory, BUPT. Her current interests include spreading dynamics and network security.

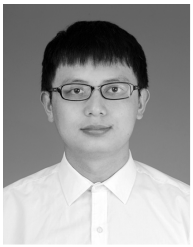

Junjie Liu was born in 1996. He received the B.S. degree in Chongqing University of Posts and Telecommunications. He is an graduate student with the School of Information and Communication Engineering, Beijing University of Posts and Telecommunications, Beijing, China. His main research interests include Internet of Vehicle, Blockchain system and Deep Reinforcement Learning.

Qimei Cui (Senior Member, IEEE) received the B.E. and M.S. degrees in electronic engineering from Hunan University, Changsha, China, in 2000 and 2003, respectively, and the Ph.D. degree in information and communications engineering from the Beijing University of Posts and Telecommunications (BUPT), Beijing, China, in 2006. She has been a Full Professor with the School of Information and Communication Engineering, BUPT, since 2014. She was a Guest Professor with the Department of Electronic Engineering, University of Notre Dame, Notre Dame, IN, USA, in 2016. Her main research interests include spectral-efficiency or energy efficiency-based transmission theory and networking technology for 4G/5G broadband wireless communications and green communications. She is a Technical Program Committee Member of several international conferences, such as the IEEE ICC, IEEE GLOBECOM, IEEE WCNC, IEEE PIMRC, IEEE/CIC ICCC, and IEEE WCSP 2013. She was a recipient of the Best Paper Award at APCC 2018, the Best Paper Award at the IEEE ISCIT 2012, the Best Paper Award at the IEEE WCNC 2014, the Honorable Mention Demo Award at the ACM MobiCom 2009, and the Young Scientist Award at the URSI GASS 2014. She is an Editor for the Science China Information Sciences, a Guest Editor for the EURASIP Journal on Wireless Communications and Networking and the International Journal of Distributed Sensor Networks.

Xiaofeng Tao (Senior Member, IEEE) received the B.S. degree in electrical engineering from Xi'an Jiaotong University, Xi'an, China, in 1993, and the M.S. and Ph.D. degrees in telecommunication engineering from Beijing University of Posts and Telecommunications (BUPT), Beijing, China, in 1999 and 2002, respectively. He is a Professor in BUPT, a Fellow of the Institution of Engineering and Technology,and Chair of the IEEE ComSoc Beijing Chapter. He has authored or co-authored over 200 papers and three books in wireless communication areas. He focuses on 5G/B5G research.

Renping Liu (Senior Member, IEEE) has supervised over 30 Ph.D. degree students. He is currently a Professor with the School of Computing and Communications, University of Technology Sydney, where he leads Network Security Lab. He is also a member of the Global Big Data Technologies Center. Prior to that, he was a Principal Scientist with CSIRO, where he led wireless networking research activities. He specializes in protocol design and modeling. He has delivered networking solutions to a number of government agencies and industry customers. He has over 100 research publications. His research interests include Markov analysis and QoS scheduling in WLAN, VANET, the IoT, LTE, 5G, SDN, and network security. He was the winner of the Australian Engineering Innovation Award and the CSIRO Chairman Medal.